Available online at www.sciencedirect.com
SCIENCE DIRECT
Journal of Power Sources 158 (2006) 557–563
JOURNAL OF POWER SOURCES
www.elsevier.com/locate/jpowsour

# Silicon and carbon based composite anodes for lithium ion batteries

Moni Kanchan Datta [a], Prashant N. Kumta [a,b,*]

[a] *Department of Materials Science and Engineering, Carnegie Mellon University, Pittsburgh, PA 15213, USA*
[b] *Department of Biomedical Engineering, Carnegie Mellon University, Pittsburgh, PA 15213, USA*

Received 25 July 2005; received in revised form 6 September 2005; accepted 8 September 2005
Available online 10 November 2005

**Abstract**

Composites comprising silicon (Si), graphite (C) and polyacrylonitrile-based disordered carbon (PAN-C), denoted as Si/C/PAN-C, have been synthesized by thermal treatment of mechanically milled silicon, graphite, and polyacrylonitrile (PAN) powder of nominal composition C–17.5 wt.% Si–30 wt.% PAN. PAN acts as a diffusion barrier to the interfacial diffusion reaction between graphite and Si to form the electrochemically inactive SiC during prolonged milling of graphite and Si, which could be easily formed in the absence of PAN. In addition, graphite, which contributes to the overall capacity of the composite and suppresses the irreversible loss, retains its graphitic structure during prolonged milling in the presence of PAN. The resultant Si/C/PAN-C based composites exhibit a reversible capacity of ∼660 mAh $g^{-1}$ with an excellent capacity retention displaying almost no fade in capacity when cycled at a rate of ∼C/4. Scanning electron microscopy (SEM) analysis indicates that the structural integrity and microstructural stability of the composite during the alloying/dealloying process appear to be the main reasons contributing to the good cyclability observed in the above composites.


*Keywords:* Mechanical alloying; Si/C composite; Anode; Li ion battery

## 1. Introduction

Lithium (Li) ion batteries with high energy and power density are in great demand as energy sources for a variety of advanced technologies. The current commercial lithium ion battery is based on the use of graphitic carbon anode which provides a theoretical capacity of 372 mAh $g^{-1}$ [1]. However, the demand for new compact and modern portable electronic devices make the need for higher energy density power sources even more critical. Lithium storage anodes based on the alloying of lithium with metals and metalloids such as Sn, Si, Al and Sb are attractive alternatives to graphite due to their low cost and high energy densities, which are up to an order of magnitude higher than that of graphitized carbon [2,3]. However, the severe crystallographic volume changes that occur during the lithium alloying and dealloying processes lead to mechanical failure of the anode resulting in crumbling of the electrodes [2–4]. This effect seriously compromises the cycling efficiency and cycle life of Li ion cells due to the loss of electronic particle to particle contact and increase in electrical resistivity. Considerable effort has been made to overcome this limitation of intermetallic electrodes by using composite materials, in which an electrochemically active phase is homogeneously dispersed within an electrochemically inactive matrix [5–8]. The electrochemically inactive phase is preferred to be comprised of a soft and ductile matrix of sufficient volume fraction (∼60–70%), which can accommodate the mechanical stresses/strains experienced by the active phase and, as a result, the structural integrity of the composite electrode can be retained during the alloying and dealloying processes.

In recent years, several authors have reported [9–16] that the Si/C based composites, prepared using high energy mechanical milling and/or decomposition of organic precursors, show higher reversible capacity with respect to graphite and better capacity retention with respect to pure silicon. Yang et al. [9] have reported that silicon and graphite based composite synthesized by thermal pyrolysis of polyvinyl chloride dispersed with nanosized silicon and fine graphite particles shows a reversible capacity ∼700 mAh $g^{-1}$ with better cyclability than nanocrystalline Si alone. Composites based on Si and disordered carbon, synthesized by pyrolyzing pitch and polysilane blends, shows a reversible capacity ∼500 mAh $g^{-1}$ with good cyclability

* Corresponding author. Tel.: +1 412 268 8739; fax: +1 412 268 7596.
*E-mail address:* kumta@cmu.edu (P.N. Kumta).

0378-7753/$ – see front matter © 2005 Elsevier B.V. All rights reserved.
doi:10.1016/j.jpowsour.2005.09.016

[10]. However, Si/C composite synthesized by decomposition of organic precursors shows a large irreversible loss in the first cycle due to the formation of disordered carbon, porosity, and/or presence of hydrogen/oxygen/sulfur in the final product. On the other hand, Si/C composite, synthesized by moderate ball milling of carbon (graphite, MCMB, disordered carbon, etc.) and nanocrystalline Si [14–16] shows a high first discharge and charge capacity (~800–1400 mAh $g^{-1}$ depending on the compositions studied) but exhibits poor capacity retention which is not suitable for practical commercial applications. Gross et al. [15] have reported that the Si/C composite, synthesized by mechanical mixing of graphite and premilled Si powder for a period of about 15 min by using Spex 8000 shaker mill, shows a first charge capacity ~800 mAh $g^{-1}$ with a fade in capacity ~1.25% (~600 mAh $g^{-1}$ after 20 cycles) of nominal composition C–20 wt.% Si. The poor capacity retention may arise not only due to Si being not homogeneously distributed in the carbon matrix, but also due to poor interface adhesion between carbon and Si during the short duration of milling. In this regard, extended milling could be useful to disperse the active Si phase homogeneously in the graphite matrix resulting in good capacity retention of the Si/C composite. However, the formation of the undesired SiC and amorphization of graphite during prolonged milling (e.g. within ~5 h of milling in Spex 8000 shaker mill) of graphite and Si [6,15–18] limits the feasibility of mechanical milling to synthesize Si/C composites for possible application as an anode in the Li ion battery industry.

We have recently identified that the addition of soft metal (e.g. Sn) or certain polymers act as a diffusion barrier to the reaction between Si and graphite to form SiC during extended milling [18]. In the present study, polyacrylonitrile (PAN) has been used as a diffusion barrier to prevent the formation of SiC during prolonged milling (~15 h) using Spex 8000 shaker mill, and thus composites based on silicon and graphite, where the active Si phase is homogeneously distributed in the graphite matrix, and also coated with the thermally decomposed product of PAN has been proposed as suitable anode materials for probable use as anodes for lithium ion batteries. The composite exhibits high reversible capacity and excellent capacity retention with ~26% irreversible loss in the first cycle. Results of these studies are presented and described in the present manuscript.

## 2. Experimental details

### 2.1. Materials synthesis

Mixtures of elemental powders of synthetic graphite (Aldrich, 1–2 μm), Si (Alfa aesar, −325 mesh) and PAN (Aldrich) of elemental composition 70 wt.% [C–25 wt.% Si]–30 wt.% PAN which is equivalent to the elemental composition of C–17.5 wt.% Si–30 wt.% PAN were subjected to mechanical milling in a high energy shaker mill (SPEX CertiPrep 8000 M) up to 15 h in a stainless steel (SS) vial using 20 SS balls of 2 mm diameter (~20 g) with a ball to powder weight ratio 10:1. Specifically, 0.6 g of PAN was dissolved in ~10 ml *N*-methylpyrrolidinone (NMP) to form a homogeneous solution. Graphite (~1.05 g), Si (~0.35 g), and the PAN solution were batched in a vial inside an argon filled glove box (~10 ppm oxygen and ~0.10 ppm moisture) in order to prevent oxidation of the reactive components during milling. The PAN solution keeps the ingredients and grinding balls completely submerged. This was helpful to avoid excessive cold welding, agglomeration and temperature build up during milling. In order to decompose PAN to form PAN-based carbon (PAN-C) [19], the mechanically milled powders were annealed isothermally at 1073 K for 4 h in an ultrahigh purity argon (UHP-Ar) atmosphere using a heating rate of 10 K $min^{-1}$ and a flow rate of 100 mL $min^{-1}$. In order to understand the effect of PAN on the phase formation and the ensuing electrochemical properties, milling has also been performed on graphite and Si of nominal composition C–25 wt.% Si in the absence of PAN using similar milling conditions.

### 2.2. Materials characterization

To identify the phase constitution, the milled powders as well as heat treated powders were characterized by X-ray diffraction (XRD) using the Philips XPERT PRO system employing the Cu Kα ($\lambda = 0.15406$ nm) radiation. In order to identify the decomposition temperature and the yield of PAN, differential thermal analysis (DTA) and thermo gravimetric analysis (TGA) has been performed for pure PAN. The DTA/TGA experiments were performed in a simultaneous TGA/DTA machine (TA 2960, TA Instrument, New Castle, DE) under UHP-Ar at a heating rate of 10 K $min^{-1}$ using ~13.5 mg PAN. To investigate the microstructure of the as prepared composites as well as electrochemically-cycled sample, scanning electron microscopy (SEM) analysis was conducted. Philips XL30 operating at 20 kV was employed for the SEM observation. In order to evaluate the electrochemical characteristics, electrodes were fabricated by mixing 82 wt.% of the active powder of −325 mesh and 8 wt.% acetylene black. A solution containing 10 wt.% polyvinylidene fluoride (PVDF) in *N*-methylpyrrolidinone was added to the mixture. The as-prepared solution was coated onto a Cu foil. A 2016 coin cell design was used employing lithium foil as an anode and 1 M LiPF6 in ethylene carbonate/diethyl carbonate (EC/DEC = 2:1 in volume) as the electrolyte. All batteries tested in this study were cycled in the voltage range from 0.02 to 1.2 V employing a constant current of 160 mA $g^{-1}$ and a minute rest period between the charge/discharge cycles using a potentiostat (Arbin electrochemical instrument).

## 3. Results and discussion

Fig. 1 shows the XRD patterns obtained from graphite–25 wt.% Si after milling for different time periods (thereafter the milled powder will be denoted as Si/C). Within 2 h of milling, the crystalline graphite structure collapses to an amorphous form, which is expected to arise due to the defect-induced melting of crystalline graphite above the critical lattice strain [20,21]. Formation of nanocrystalline SiC of crystallite size ~10 nm, calculated from the most intense peak

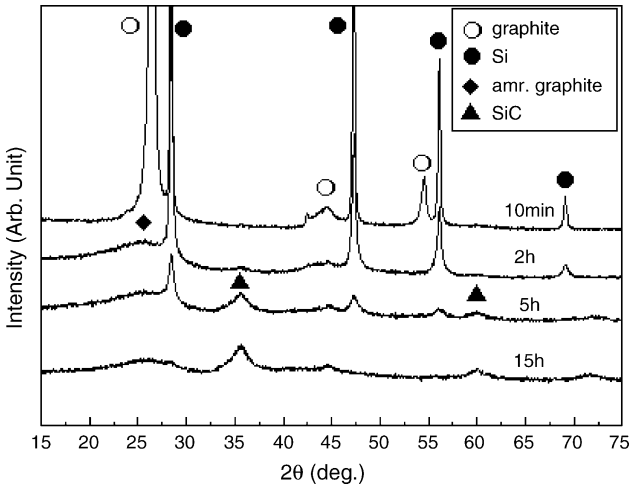


Fig. 1. XRD patterns of C–25 wt.% Si composite generated after milling for different time intervals.

of SiC using the Voigt function of single line approximation method [21,22], has been identified after 5 h of milling. With increasing milling time, the weight fraction of SiC increases whereas the weight fraction of the active Si phase decreases. After 15 h of milling, almost all the Si has been consumed, and the final product has been identified as a mixture of amorphous graphite and nanocrystalline SiC as expected from the equilibrium phase diagram [23].

Fig. 2 shows the variation of specific capacity versus cycle number for the Si/C composite obtained after 10 min, 2 and 5 h of milling, cycled at a rate of 160 mA $g^{-1}$. As shown in Fig. 2, the first discharge and charge capacity of Si/C decreases with increasing milling time which clearly suggests that the weight fraction of the active Si phase decreases with increasing milling time, which is in good agreement with the XRD result. On the other hand, the irreversible loss in the first cycle for the Si/C, plotted in Fig. 3, increases significantly with increasing milling time, which is expected as a result of the increasing solid–electrolyte interphase reaction occurring due to a greater refinement of the

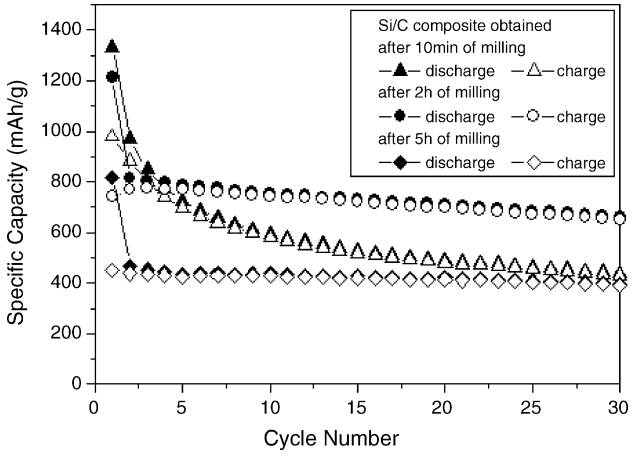


Fig. 2. Specific capacity vs. cycle numbers of C–25 wt.% Si obtained after milling for different time intervals, and cycled at a constant current of 160 mA $g^{-1}$.

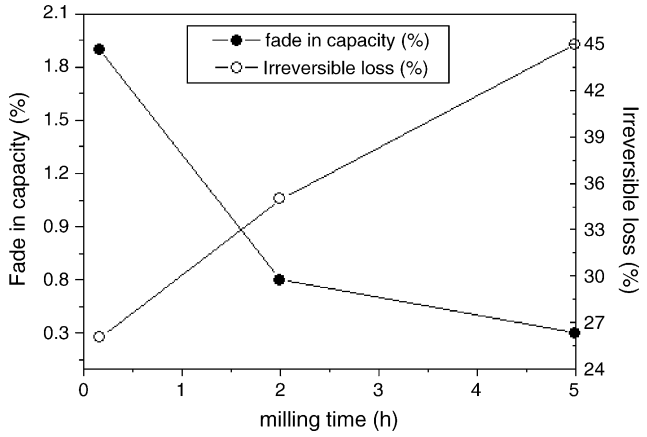


Fig. 3. Variation in fade in capacity (%) and irreversible loss of C–25 wt.% Si obtained after milling for different time intervals.

particle size of the respective phases with increasing milling time. In addition, the formation of amorphous graphite after 2 h of milling (Fig. 1), which is known to react with Li irreversibly [24], probably contributes to the significantly high irreversible loss of Si/C obtained after prolonged milling. The overall percentage fade in capacity of Si/C as a function of milling time has also been plotted in Fig. 3. The retention in capacity improves significantly after 2 h of milling in comparison to 10 min of milling. For example, the sample milled for 2 and 5 h shows an overall fade in capacity of 0.6 and 0.3% loss per cycle, respectively, whereas the sample milled for only 10 min fades at a rate of 1.9% loss per cycle. However it must be noted that the Si/C obtained after 10 min of milling shows a rapid fade in the early stage of cycling (∼4% fade per cycle up to 10 cycles), which gradually stabilizes (∼1.0% loss per cycle after 20 cycles) close to the capacity of graphite (Fig. 2). This result clearly suggests that the Si particles are pulverized at the early stage of alloying and dealloying processes, whereas graphite maintains its structural integrity. In other words, it can be concluded that the Si and graphite in Si/C obtained after 10 min of milling exist as separate entities and distinct phases rather than forming a true composite. On the other hand, the Si/C obtained after 2 and 5 h of milling shows a fade in capacity of 0.6 and 0.3%, respectively, throughout the cycling test without exhibiting any rapid fade in the early stage of cycling, which suggest that these systems exhibit characteristics of a homogeneous composite rather than existing as separate entities due to the more homogeneous distribution of Si in graphite, and possible formation of some interface bonding occurring between graphite and Si.

The above results clearly suggest that extended milling is useful to induce capacity retention leading to enhanced cycle life due to silicon that is more homogeneously distributed in the graphite matrix. At the same time, the extended milling also probably induces a good interface adhesion between the Si and graphite. However, in order to obtain the high capacity and low irreversible loss with good cyclability in Si/C based composite, it is of paramount importance to circumvent the formation of SiC during extended milling of graphite and Si, and also reduce the kinetics of amorphization of graphite. In order to

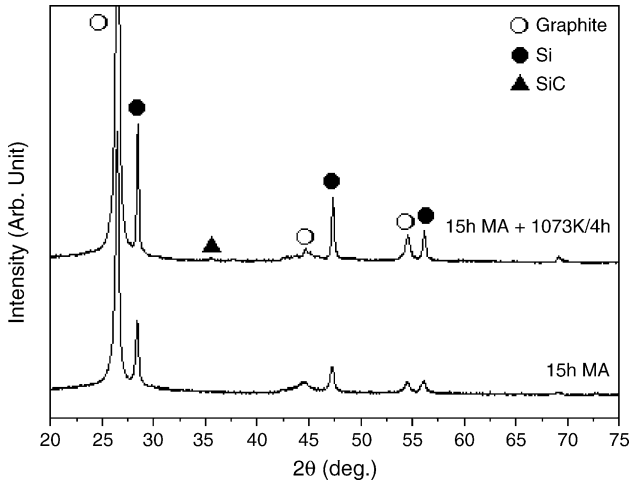


Fig. 4. XRD patterns of C–17.5 wt.% Si–30 wt.% PAN generated after 15 h of milling and after thermal treatment at 1073 K for 4 h following the 15 h of milling.

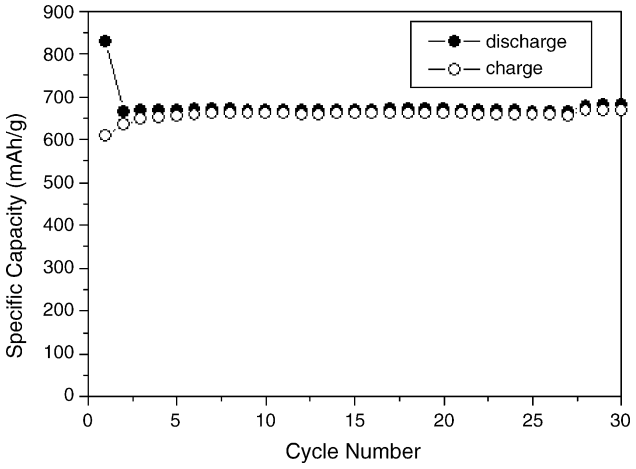


Fig. 6. Specific capacity vs. cycle number of C/Si/PAN-C derived composite electrode cycled at a rate of 160 mAh $g^{-1}$.

achieve this, mechanical milling of graphite and Si has been performed in the presence of PAN which is expected to act as a diffusion barrier between Si and graphite to circumvent the formation of SiC. Fig. 4 shows the XRD patterns of C–17.5 wt.% Si–30 wt.% PAN milled for 15 h. In contrast to C–25 wt.% Si (Fig. 1), XRD patterns of C–17.5 wt.% Si–30 wt.% PAN milled for 15 h shows only the presence of graphite and Si without any detectable amount of SiC. It is interesting to note that with the addition of PAN, the amorphization of graphite is also reduced, retaining its desired graphitic structure even after 15 h of milling.

In order to identify the decomposition temperature and weight loss of PAN, DTA/TGA has been performed for pure PAN. The DTA curve of pure PAN, shown in Fig. 5, shows a sharp exothermic peak at about 568 K, whereas the TGA result (Fig. 5) shows a significant weight loss (∼57%) in the temperature region 553–773 K which corresponds to the decomposition of PAN to PAN-based carbon. The TGA curve also shows a ∼13.8% weight loss in the temperature range 773–1073 K which mainly arises due to the removal of hydrogen/nitrogen species from PAN-C. It has been reported that the residual hydrogen and nitrogen are completely removed only above 1273 and 1773 K, respectively [19,25]. However, in the present experiment, it has been identified that SiC begins to form when the milled powder is thermally treated above 1073 K. Based on the DTA/TGA results, the milled powder has been thermally treated at 1073 K for 4 h in UHP-Ar atmosphere to decompose PAN to form PAN-derived carbon. The XRD patterns of thermally treated powder, shown in Fig. 4, show the peaks corresponding to graphite and Si with negligible amount of SiC. The thermally treated powder of C–17.5 wt.% Si–30 wt.% PAN thereafter will be denoted as Si/C/PAN-C composite. The composition of the Si/C/PAN-C composite is estimated based on the 37% yield of PAN-C and no weight loss of Si and graphite observed from thermal analysis to be approximately C–21.6 wt.% Si–13.6 wt.% PAN-C.

Fig. 6 shows the variation of specific capacity versus cycle number of Si/C/PAN-C cycled at a constant current of 160 mA $g^{-1}$. The discharge/charge profiles of Si/C/PAN-C composite, shown in Fig. 7, indicates that at the above rate the electrode requires ∼4 h for completing one half cycle which

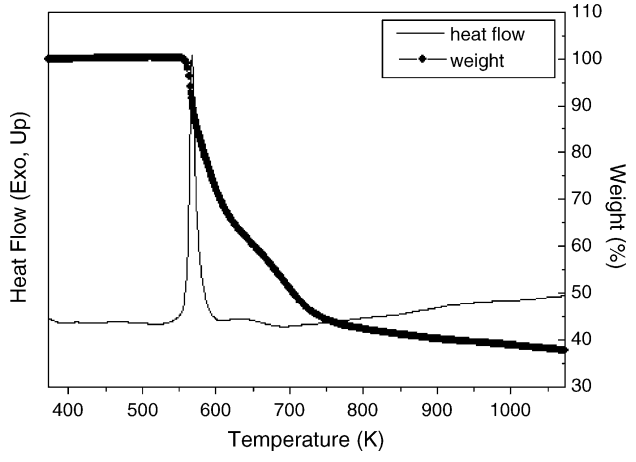


Fig. 5. DTA/TGA traces of pure PAN conducted in ultra high purity Argon.

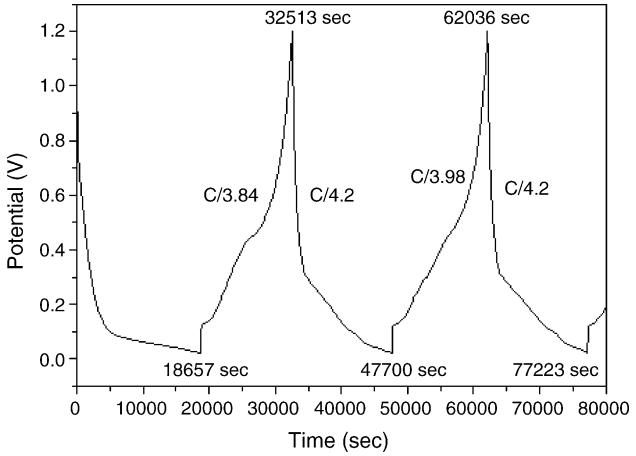


Fig. 7. The discharge/charge profiles of Si/C/PAN-C composite electrode cycled at a constant current of 160 mA $g^{-1}$.

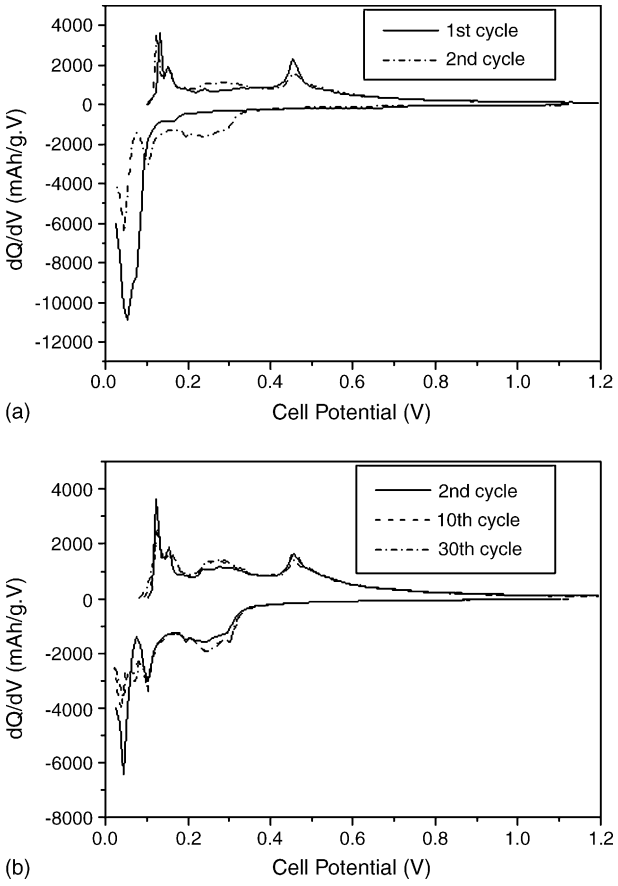


Fig. 8. Differential capacity vs. cell potential curves of C/Si/PAN-C derived composite electrode (a) after 1st and 2nd cycle and (b) after 2nd, 10th and 30th cycle.

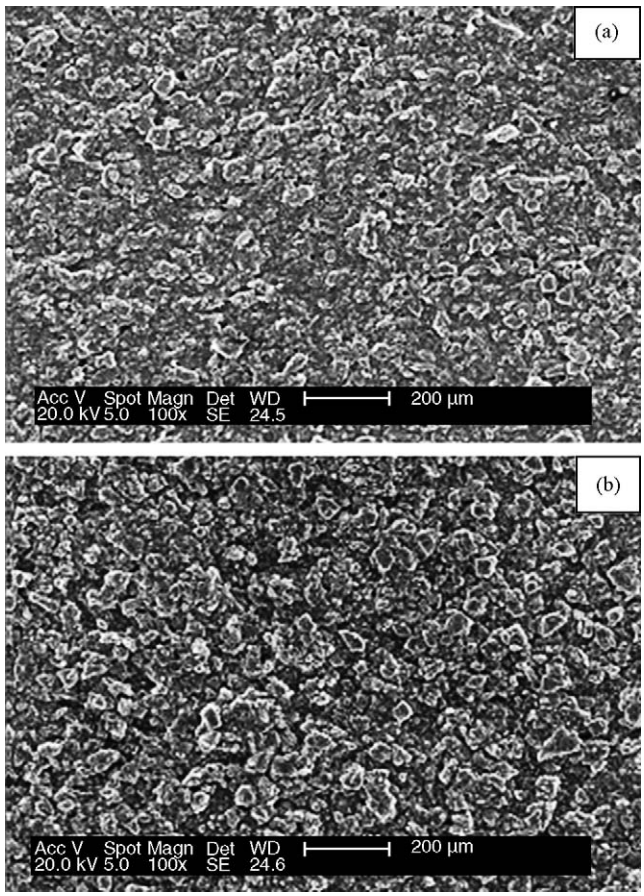


Fig. 9. SEM micrograph of Si/C/PAN-C electrode (a) before and (b) after cycling for 30 cycles.

corresponds to a rate of ∼C/4. The Si/C/PAN-C composite shows a first discharge and first charge capacity ∼825 and ∼610 mAh $g^{-1}$, respectively, with an irreversible loss of ∼26%. The irreversible loss of Si/C/PAN-C composite is comparable to the Si/C obtained after 10 min of milling, whereas it is significantly lower in comparison to 2 and 5 h milled Si/C (Fig. 3). The low irreversible loss of Si/C/PAN-C composite in comparison to Si/C obtained after 2 and 5 h of milling is expected as a result of the retention of the graphitic structure in the Si/C/PAN-C composite. As shown in Fig. 6, the reversible capacity increases with subsequent cycles and after the fifth cycle the Si/C/PAN-C composite exhibits an optimal reversible capacity ∼660 mAh $g^{-1}$ with excellent capacity retention of almost no fade in capacity up to 30 cycles. The differential capacity plot of Si/C/PAN-C composite (Fig. 8a) shows that both Si and graphite are active. In addition, the appearance of peaks corresponding to ∼0.09, ∼0.24 and ∼0.29 V after the first cycle suggest that the crystalline Si transforms to amorphous Si after the first cycle. After the first cycle, the peak intensity corresponding to the reaction of Li ion with amorphous Si (∼0.09, ∼0.24and ∼0.29 V) remains almost unchanged with cycling (Fig. 8b) which suggests the excellent retention of capacity of the composite with cycling.

The excellent capacity retention of the Si/C/PAN-C composite observed is probably due to the maintenance of the structural integrity of the electrode during the alloying and dealloying processes. The SEM micrograph of the uncycled and cycled samples of Si/C/PAN-C composite, shown in Fig. 9, indicates the excellent structural integrity (devoid of any cracks) even after 30 cycles. Moreover, there appears to be no significant change in the particle size and particle morphology after cycling, which indicates no new surfaces generated during cycling. There is in general, however, a certain degree of faceting of the featureless regions in Fig. 9a probably occurring due to some extent of coalescence of Si rich species. On the other hand, the SEM micrograph of Si/C obtained after 2 h milling (Fig. 10) shows the structural failure of the electrode during the alloying/dealloying process indicative of one of the main causes of the fade in capacity observed in this composite. The excellent structural integrity of the Si/C/PAN-C is expected to arise due to the more homogeneous distribution of Si within the graphite matrix during extended milling. In addition, the solution coating by PAN is expected to enhance the wettability between graphite and Si, and as a result, the coating by PAN-C obtained by thermal decomposition of PAN may improve the mechanical properties of the composite by enhancing the interface adhesion/bonding between Si and graphite. Thus, the PAN-based carbon coating is expected to improve the capacity retention due to enhancement of the interface strength between graphite and silicon. Further studies are necessary to clearly delineate the exact role of PAN during mechanical milling and thermal decomposition. These

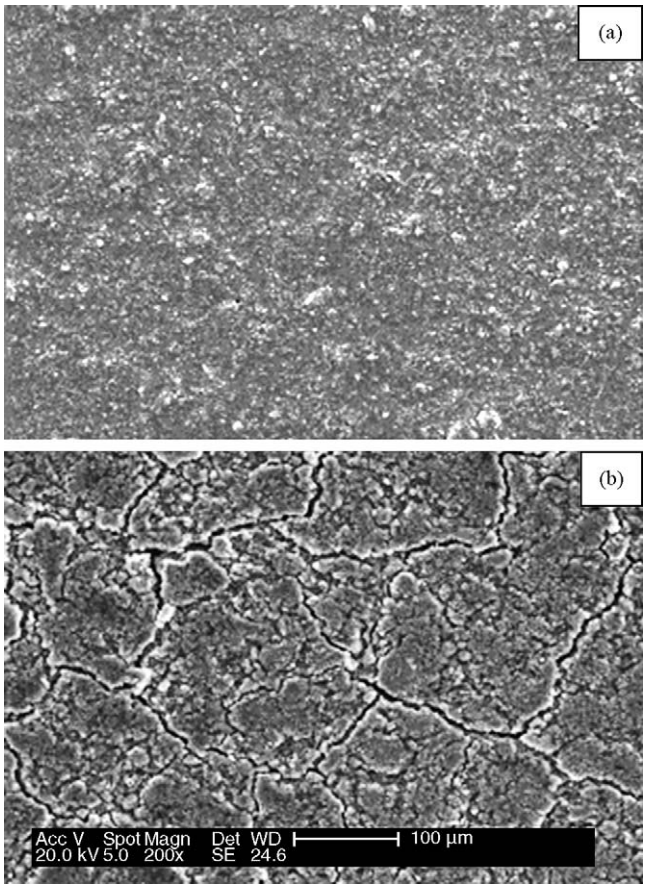


Fig. 10. SEM micrograph of Si/C electrode fabricated using S/C obtained after 2 h of milling (a) before and (b) after cycling for 30 cycles.

studies are currently ongoing and will be the subject of subsequent publications. Nevertheless, based on the above results, it can be concluded that the Si/C/PAN-C composite prepared from graphite, Si and PAN by mechanical milling followed by thermal treatment is promising for use as anodes for Li ion battery application.

## 4. Conclusion

Composites based on graphite and Si have been synthesized by prolonged mechanical milling of 15 h of graphite and Si using high energy SPEX 8000 shaker mill to ensure that Si is homogeneously distributed within the graphite matrix. However, the formation of the electrochemically inactive SiC after 5 h of milling of graphite and Si, of nominal composition C–25 wt.% Si, decreases the weight fraction of active Si, and as a result the Si/C composite obtained beyond 5 h of milling shows significantly lower reversible capacity than the Si/C composite obtained after moderate milling time of 10 min and 2 h. In order to circumvent the formation of undesired SiC during extended milling of graphite and Si, polyacronitrile (PAN) solution in NMP has been used along with graphite and Si of nominal composition C–17.5 wt.% Si–30 wt.% PAN. PAN solution in NMP acts as a diffusion barrier to the interfacial diffusion reaction between Si and graphite to form SiC during extended milling of 15 h, and as result a homogeneous distribution of Si in graphite is obtained without any detectable amount of SiC. In addition, graphite, which transform to an amorphous structure in the early stage of milling (∼2 h) in the absence of PAN, retains its graphitic structure during extended milling of 15 h in the presence of PAN. The mechanically milled powder of nominal composition C–17.5 wt.% Si–30 wt.% PAN, obtained after 15 h of milling, was thermally treated at 1073 K to decompose PAN to form PAN-based disordered carbon (PAN-C), and as a result, a composite based on graphite and Si coated with PAN-C has been synthesized. Based on the DTA/TGA results, the composition of the Si/C/PAN-C composite is estimated to be approximately C–21.6 wt.% Si–13.6 wt.% PAN-C. The resultant Si/C/PAN-C based composites exhibit a reversible capacity of ∼660 mAh $g^{-1}$ with an irreversible loss ∼26% when cycled at a current rate ∼160 mA $g^{-1}$ which is equivalent to a rate of C/4. This composite also shows an excellent capacity retention of almost no fade in capacity up to 30 cycles. SEM investigation of cycled electrode indicates that the electrode maintains its microstructure and structural integrity during discharge/charge processes.

## Acknowledgements

The authors would like to thank NSF (Grants CTS-9700343 and CTS-0000563), NASA (NAG3-2640) Mitsubishi (Japan), and ONR (N00014-00-1-0516) for financial support of this research.

## References

[1] T. Tran, J. Feikert, X. Song, K. Kinosbita, J. Electrochem. Soc. 142 (1995) 3297.
[2] J.L. Tirado, Mater. Sci. Eng. R. 40 (2003) 103.
[3] M. Winter, J.O. Besenhard, Electrochim. Acta 45 (1999) 31.
[4] C. Wang, A.J. Appleby, F.E. Little, J. Power Sources 93 (2001) 174.
[5] O. Mao, R.L. Turner, I.A. Courtney, B.D. Fredericksen, M.I. Buckett, L.J. Krause, J.R. Dahn, Electrochem. Solid-state Lett. 2 (1999) 3.
[6] Il-seok Kim, G.E. Blomgren, P.N. Kumta, J. Power Sources 130 (2004) 275.
[7] Il-seok Kim, P.N. Kumta, G.E. Blomgren, Electrochem. Solid-State Lett. 3 (2000) 493.
[8] Il-seok Kim, G.E. Blomgren, P.N. Kumta, Electrochem. Solid-State Lett. 6 (2003) A157.
[9] J. Yang, B.F. Wang, K. Wang, Y. Liu, J.Y. Xie, Z.S. Wen, Electrochem. Solid-State Lett. 6 (2003) A154.
[10] D. Larcher, C. Mudalige, A.E. George, V. Porter, M. Gharghouri, J.R. Dahn, J. Power Sources 122 (1999) 71.
[11] H. Li, X. Huang, L. Chen, Z. Wu, Y. Liang, Electrochem. Solid-State Lett. 2 (1999) 547.
[12] Il-seok Kim, P.N. Kumta, J. Power Sources 136 (2004) 145.
[13] Y. Liu, K. Hanai, J. Yang, N. Imanishi, A. Hirano, Y. Takeda, Electrochem. Solid-State Lett. 7 (2004) A369.
[14] G.X. Wang, J. Yao, H.K. Liu, Electrochem. Solid-State Lett. 7 (2004) A250.
[15] K.J. Gross, J.C.F. Wang, G.A. Roberts, US. Pat. Appl. Pub. US2004/137327 A1 (2004).
[16] C.S. Wang, G.T. Wu, X.B. Zhang, Z.F. Qi, W.Z. Li, J. Electrochem. Soc. 145 (1998) 2751.
[17] M. Sherif El-Eskandarany, K. Sumiyama, K. Suzuki, J. Mater. Res. 10 (1995) 659.
[18] M.K. Datta, P.N. Kumta, Annual report, Mitsubishi Chemical Corporation, 2003.

[19] Y. Jung, M.C. Suh, H. Lee, M. Kim, S.I. Lee, S.C. Shim, J. Kwak, J. Electrochem. Soc. 144 (1997) 4279.
[20] C. Ettl, K. Samwer, Mater. Sci. Eng. A 178 (1994) 245.
[21] M.K. Datta, S.K. Pabi, B.S. Murty, J. Mater. Res. 15 (2000) 1429.
[22] T.H. de Keijser, J.I. Langford, E.J. Mittemeijer, A.B.P. Vogels, J. Appl. Crystallogr. 15 (1982) 308.
[23] R.W. Olesinski, G.J. Abbaschian, in: T.B. Massalski, H. Okamoto, P.R. Subramanian, L. Kacprzak (Eds.), Binary Alloy Phase Diagram, vol. 1, second ed., ASM International, Materials Park, Ohio, 1990, p. 882.
[24] C.S. Wang, G.T. Wu, W.Z. Li, J. Power Sources 76 (1995) 1.
[25] P.L. Walker, Chemistry and Physics of Carbon, Marcel Dekker, New York, 1971.